Table II. Surface Areas of Calcinated Al_{13}^{7+}–Tetratitanate Samples

sample	surf area, m^2/g	sample	surf area, m^2/g
AT/25/120/500	139	AT/100/1/500	176
AT/50/8/500	148	AT/100/6/500	254
AT/60/4/500	153	$K_2Ti_4O_9$[a]	58
AT/70/7/500	122		

[a] Starting material.

in the range of 10 nm. The diameter of Al_{13}^{7+} Keggin ions is ca. 9 Å, which will be the pore diameter if zeolitic pores are formed between the layers. Therefore, the observed porous structures are presumably due to defects in the structure and to void space at the boundary of different phases, considering that the crystallinity is rather poor and anatase TiO_2 forms upon calcination. Pinnavaia et al.[25] have reported that the porous structures of pillared clays are dependent upon the drying processes. This topic will be further investigated and reported in a separate paper dealing with the catalytic properties of the Al_{13}^{7+}-pillared tetratitanate.

(25) Pinnavaia, T. J.; Tzou, M.-S.; Landau, S. D.; Raythatha, R. H. *J. Mol. Catal.* **1984**, *27*, 195.

Conclusion

Our results demonstrate that layered tetratitanate compounds can be pillared with Al_{13}^{7+} Keggin ions. The resultant complex has an interlayer distance of 15.3 Å. Methods applied were not similar to those used to pillar clays. Because tetratitanates do not swell in water, the interlayer spacing has to be propped open by alkylammonium ions. The open layers then facilitate the replacement of alkylammonium ions by Al_{13}^{7+} Keggin ions. In order to avoid other cations in the solution competing for ion-exchange sites, alkylamines are used to hydrolyze $AlCl_3$. The formation of Al_{13}^{7+} Keggin ions in the alkylamine-hydrolyzed $AlCl_3$ solutions was confirmed by ^{27}Al NMR spectra. Hexylammonium ions were found more stable in maintaining the interlayer distances of tetratitanates than butylammonium ions during the exchange process. The hexylammonium tetratitanate complex, when exchanged with hexylamine-hydrolyzed $AlCl_3$ solutions, leads to the formation of an Al_{13}^{7+}-pillared complex. These pillared compounds after calcination at 500 °C demonstrate medium-sized-pore structures and have fairly high surface areas.

Acknowledgment. Financial support under Grant No. NSC76-0208-M002-39 from National Science Council of the Republic of China is gratefully acknowledged.

Contribution from the Department of Chemistry, Massachusetts Institute of Technology, Cambridge, Massachusetts 02139

Isomerization of Binuclear Amidate-Bridged Platinum(II) Amine Complexes: A ^{195}Pt NMR Investigation

Thomas V. O'Halloran and Stephen J. Lippard*

Received July 29, 1988

^{195}Pt NMR spectroscopy has been used to identify and follow the reversible stereochemical rearrangement of the head-to-head (HH) isomer of $[Pt_2(en)_2(C_5H_4NO)_2](NO_3)_2$, where en = ethylenediamine and $C_5H_4NO^-$ is the α-pyridonate anion, to form the head-to-tail (HT) isomer in aqueous solution. Kinetic studies of the reaction established the rate law to be $-d(HH)/dt = d(HT)/dt = k_f[HH] - k_r[HT]$, an approach-to-equilibrium expression for which $K_{eq} = k_f/k_r$ and $k_{obs} = k_f + k_r$. For a typical run at 39 °C and pH 6.5 in 0.04 M phosphate buffer, $k_f = 7.4\ (2) \times 10^{-5}\ s^{-1}$, $k_r = 13.9\ (2) \times 10^{-5}\ s^{-1}$, and $K_{eq} = 0.53$. Temperature-dependent rate measurements revealed $\Delta H^{\ddagger}$ and $\Delta S^{\ddagger}$ to be 114 (5) kJ mol^{-1} and 40 (10) J mol^{-1} K^{-1}, respectively, values characteristic of a dissociative rate-determining step in the reaction mechanism. The suggestion that the isomerization is dissociatively activated is supported by the failure of DMSO to accelerate the rate, as would be expected for an associative mechanism, and the fact that the *cis*-diammineplatinum(II) analogue isomerizes at least 70 times slower than the sterically hindered ethylenediamine complex. The latter result is ascribed to steric strain in the $[Pt_2(en)_2(C_5H_4NO)_2]^{2+}$ complex, a consequence of nonbonded interactions between the hydrocarbon chains of the ethylenediamine ligands in two adjacent coordination planes. The isomerization reaction was shown to be intramolecular by the failure of added 6-methyl-α-pyridone or $[Pt(en)(H_2O)_2]^{2+}$ to affect the rate of product distribution. A mechanism is presented in which Pt–N(α-pyridonate) bond breaking is postulated to occur in the HH → HT rearrangement process.

Introduction

Binuclear complexes bridged by two ligands are known to form in the reaction of the anticancer drug *cis*-diammineplatinum(II) (*cis*-DDP) with various amidate ligands including α-pyridone,[1,2]

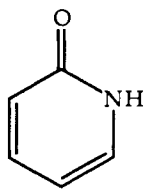

α-pyridone, C_5H_4NHO

a pyrimidine analogue, 1-methylcytosine,[3] 1-methylthymine,[4,5] 1-methyluracil,[6,7] 1-methylhydantoin,[8] 2-mercaptopyridine,[9] and α-pyrrolidone.[10] This chemistry was initially discovered in attempts to understand the interactions of the platinum(II) complexes with constituents of the proposed target of *cis*-DDP, DNA. The reactions gave rise to intensely colored blue compounds, which

(1) For a review, see: Lippard, S. J. *Science (Washington, D.C.)* **1982**, *218*, 1075.
(2) Hollis, L. S.; Lippard, S. J. *J. Am. Chem. Soc.* **1983**, *105*, 3494 and references therein.
(3) Faggiani, R.; Lippert, B.; Lock, C. J. L.; Speranzini, R. A. *J. Am. Chem. Soc.* **1981**, *103*, 1111.
(4) Lock, C. J. L.; Peresie, H. J.; Rosenberg, B.; Turner, G. J. *J. Am. Chem. Soc.* **1978**, *100*, 3371.
(5) Lippert, B.; Neugebauer, D.; Schubert, U. *Inorg. Chim. Acta* **1980**, *46*, L11.
(6) Faggiani, R.; Lock, C. J. L.; Rosenberg, B.; Turner, G. *Inorg. Chem.* **1981**, *20*, 804.
(7) Lippert, B. *Inorg. Chem.* **1981**, *20*, 4326.
(8) Laurent, J.-P.; Lepage, P.; Dahan, P. *J. Am. Chem. Soc.* **1982**, *104*, 7335.
(9) Kinoshita, I.; Yasuba, Y.; Matsumoto, K.; Doi, S. *Inorg. Chim. Acta* **1983**, *80*, L13.
(10) Matsumoto, K. *Chem. Lett.* **1984**, 2061.

0020-1669/89/1328-1289$01.50/0 © 1989 American Chemical Society

themselves had antitumor properties.[11,12] Subsequent studies revealed one of these blue compounds to be a paramagnetic platinum cluster composed of two α-pyridonate-bridged binuclear units bound together by metal–metal and hydrogen-bonding interactions. Studies on *cis*-diammineplatinum α-pyridone blue, the first blue crystalline platinum to be characterized, have provided extensive insight into the nature of the platinum pyrimidine blues.[12-14]

Following an investigation of the ^{195}Pt NMR properties of one class of binuclear Pt(II) complexes bridged by two α-pyridonate ligands,[15] we discovered an unusually facile stereochemical rearrangement of the head-to-head isomer of $[Pt_2(en)_2(C_5H_4NO)_2](NO_3)_2$ to form the head-to-tail isomer.[16] This isomerization required a typically inert Pt–N(heterocycle) bond trans to an amine to be cleaved with a half-life of hours at room temperature. Since the antitumor properties of platinum ammine complexes result from platinum binding to the heterocyclic nitrogen bases of DNA, forming bonds that are typically inert, rearrangements of this kind are potentially relevant to the mechanism of action of *cis*-DDP. We therefore undertook a detailed mechanistic study of this isomerization to elucidate factors that affect the Pt–N bond lability. Here we present full details of our work on $[Pt_2(en)_2(C_5H_4NO)_2](NO_3)_2$, a preliminary account of which was communicated previously.[16] Rearrangements have also been observed for a family of α-pyridonate-bridged binuclear *cis*-dimethylplatinum(III) complexes, but no thermodynamic or mechanistic information is yet available.[17]

Experimental Section

Preparation of Compounds. Starting materials $[Pt(NH_3)_2I_2]$ and $[Pt(en)I_2]$ were prepared from recrystallized $K_2[PtCl_4]$ (Engelhard).[2,15] α-Pyridone (Aldrich) was recrystallized twice from toluene, and 6-methyl-α-pyridone (Aldrich) was used as provided. All other reagents were obtained from commercial sources.

The head-to-head isomer of $[Pt_2(en)_2(C_5H_4NO)_2](NO_3)_2$ (**1**) was prepared by adding 1 equiv of α-pyridone to $[Pt(en)(OH_2)_2]^{2+}$ and raising the pH to 6 with NaOH, as reported previously.[15] The head-to-head isomer of $[Pt_2(NH_3)_4(C_5H_4NO)_2](NO_3)_2$ (**3**)[2] was prepared by reducing *cis*-diammineplatinum α-pyridone blue with ascorbic acid under N_2, to prevent reoxidation to the blue species. The head-to-tail isomer of $[Pt_2(NH_3)_4(C_5H_4NO)_2](NO_3)_2 \cdot 2H_2O$ (**4**) was isolated from the α-pyridone blue reaction as previously reported.[2] The head-to-tail (ethylenediamine)platinum(II) complex, $[Pt_2(en)_2(C_6H_6NO)_2](NO_3)_2$ (**5**), which is bridged by two 6-methyl-α-pyridonate ligands, was prepared by adding 54.9 mg (0.5 mmol) of 6-methyl-α-pyridone to 0.56 mmol of $[Pt(en)(OH_2)_2](NO_3)_2$ in a total volume of 10 mL. The pH was adjusted from 2.5 to 6.3 by adding 1 M NaOH. After being heated at 36 °C for several days, the solution was allowed to evaporate in the air, yielding ~0.1 g (50%) of opaque tan needles. Anal. Calcd for $[Pt(en)(C_6H_6NO)]_2(NO_3)_2 \cdot 2H_2O$ ($Pt_2C_{16}H_{32}N_8O_{10}$): C, 21.67; H, 3.64; N, 12.64. Found: C, 21.44, 21.40; H, 3.34, 3.36; N, 12.49, 12.46. The purity of these samples was further assessed by ^{195}Pt NMR spectroscopy, which revealed only one peak for head-to-tail (HT) complexes and two ^{195}Pt peaks for head-to-head (HH) complexes in the range −1000 to −2800 ppm.

Kinetic Measurements. All rates were measured in potassium phosphate buffer, pH 6.5, μ = 60 mM, unless otherwise specified. The temperature of the 20-mm sample tube (containing 10 mL of solution) was maintained by a Bruker thermostated air-flow system. Temperature measurements were made by immersing a thermometer in the sample immediately upon its removal from the coil. NMR tubes were routinely spun at 4 Hz to minimize vigorous vortexing but allow circulation of liquid in the large 20-mm tube.

Acquisition of ^{195}Pt NMR Spectra. ^{195}Pt NMR spectra were acquired on either a Bruker WM-300 spectrometer operating at 64.3 MHz with a 20-mm fixed-frequency probe (90° ≈ 90 μs) or a Bruker WM-250 spectrometer operating at 53.68 MHz with a 10-mm fixed-frequency probe (90° ≈ 26 μs). All spectra used in kinetic analyses were acquired on the WM-300 instrument. Typically, 75 000 transients were accumulated per kinetics spectrum, using 1K of memory with a 100-kHz spectral width and a 25-μs pulse width. The FTQ NMR software, using these acquisition parameters, imposed either an 8.3- or 25.2-ms real repetition rate when spectral acquisition was automated. A delay equal to the time required to obtain one spectrum (real repetition rate multiplied by the number of transients) was utilized between the acquisition of subsequent spectra in a given kinetics run. Typically, a run consisted of 20 spectra acquired over at least 3 half-lives. The time point assigned to a given spectrum was the midpoint of the acquisition.

Data Treatment. Peak heights at given times were fit to rate equations by using a nonlinear least-squares program and unit weights. All correlation coefficients were greater than 0.99 unless otherwise noted.

Equilibrium Measurements. After a kinetics run, samples were incubated for approximately 20 half-lives at the specified temperature, following which time a spectrum of the system at equilibrium was measured. These spectra were typically the sum of 200 000 transients accumulated in 1K of memory by using a 5-μs pulse width and a 100-kHz spectral width. Equilibrium constants were calculated from the integrated peak areas. Since head-to-tail complexes contain two chemically identical platinum nuclei per molecule, half of this peak area was employed in these calculations.

Table I. Chemical Shifts of Platinum(II) α-Pyridonate Complexes

compd no.	cation	Pt ligands	$-\delta(^{195}Pt)^a$	$10^4T_2^*$, s^b
1	HH-$[Pt_2(en)_2(C_5H_4NO)_2]^{2+}$	N_2O_2	1610.5	4.8
		N_2N_2	2480.3	3.4
2	HT-$[Pt_2(en)_2(C_5H_4NO)_2]^{2+}$	$N_2N'O$	2055.8	
3	HH-$[Pt_2(NH_3)_4(C_5H_4NO)_2]^{2+}$	N_2O_2	1306.9[c]	
		N_2N_2	2261.8[c]	
4	HT-$[Pt_2(NH_3)_4(C_5H_4NO)_2]^{2+}$	$N_2N'O$	1808.6[c]	
5	HT-$[Pt_2(en)_2(C_6H_6NO)_2]^{2+}$	$N_2N'O$	2030.8[e]	
6	$[Pt(en)(OH_2)_2]^{2+}$	N_2O_2	1835[d]	
7	$[Pt(en)(C_5H_4NO)(OH_2)]^{2+}$	$N_2N'O$	2316[d]	
8	$[Pt(en)(C_5H_4NO)_2]^{2+}$	$N_2N'_2$	2685[d]	

[a] ^{195}Pt NMR chemical shifts measured at pH 6.5 were referenced to $K_2[PtCl_6]$. [b] Calculated from line widths at half-height for given peak at 53.68 MHz. [c] See ref 2 for further discussion. [d] pH 2.0. These compounds have a pH-dependent chemical shift, as expected for complexes with acidic protons. [e] 6-Methyl-α-pyridonate HT binuclear complex.

Results

^{195}Pt NMR Spectra. Fresh solutions of the structurally characterized[15] head-to-head isomer of $[Pt_2(en)_2(C_5H_4NO)_2](NO_3)_2$ exhibit two ^{195}Pt resonances separated by 870 ppm (Figure 1). The downfield resonance is assigned to the $\{Pt(en)\}^{2+}$ moiety bound to both bridging pyridonate ligands through exocyclic oxygen atoms. The other platinum nucleus is bound to both bridging ligands through their heterocyclic nitrogen atoms, giving an $N_2N'_2$ environment. These assignments (Table I) are based on established ^{195}Pt chemical shift trends. The more electronegative the substituent, the more extensively deshielded is the platinum nucleus.[18] The assignment is further corroborated by the fact that the upfield resonance, assigned to the $Pt(N_2N'_2)$ site, has a shorter T_2^* value than that of the $Pt(N_2O_2)$ site (Table I). This difference is expected for a nucleus surrounded by four versus two quadrupolar ^{14}N nuclei (^{14}N; I = 1, natural abundance 99%) in an asymmetric environment.

Over a period of several hours at room temperature, a new resonance appears that increases in intensity at the expense of the two resonances of the head-to-head isomer (**1**) (Figure 1). This new resonance occurs midway between those for platinum nuclei in N_2O_2 and $N_2N'_2$ sites. It does not correspond in chemical shift to any of the known mononuclear (ethylenediamine)platinum(II) α-pyridone complexes.[19] On the basis of these observations, the new resonance is assigned to the head-to-tail isomer of **1**, having a single $N_2N'O$ coordination environment comprising an

(11) (a) Davidson, J. P.; Faber, R. G.; Fischer, R. G., Jr.; Mansy, H. J.; Peresie, B.; Rosenberg, B.; van Camp, L. *Cancer Chemother. Rep.* **1975**, *59*, 287. (b) Rosenberg, B. *Cancer Chemother. Rep.* **1975**, *29*, 589.
(12) Barton, J. K.; Szalda, D. J.; Rabinowitz, H. N.; Waszczak, J. W.; Lippard, S. J. *J. Am. Chem. Soc.* **1979**, *101*, 1434.
(13) Barton, J. K.; Caravana, C.; Lippard, S. J. *J. Am. Chem. Soc.* **1979**, *101*, 7269.
(14) Ginsberg, A. P.; O'Halloran, T. V.; Fanwick, P. E.; Hollis, L. S.; Lippard, S. J. *J. Am. Chem. Soc.* **1984**, *106*, 5430.
(15) Hollis, L. S.; Lippard, S. J. *Inorg. Chem.* **1983**, *22*, 2600.
(16) O'Halloran, T. V.; Lippard, S. J. *J. Am. Chem. Soc.* **1983**, *105*, 3342.
(17) Bancroft, D. P.; Cotton, F. A. *Inorg. Chem.* **1988**, *27*, 1633.
(18) Pregosin, P. *Annu. Rep. NMR Spectrosc.* **1986**, *17*, 285.
(19) O'Halloran, T. V. Ph.D. Dissertation, Columbia University, 1985.

Table II. Rate and Equilibrium Data for the HH ⇌ HT Isomerization of $[Pt(en)(C_5H_4NO)]_2^{2+}$

run no.	conditions[a]	T, °C	pH[b]	K_{eq}	$10^5\ k_{obs}$,[1c] s^{-1}	$10^5\ k_{obs}$[2c] s^{-1}	$10^5\ k_{obs}$[3d] s^{-1}	$10^5\ k_f$,[f] s^{-1}	$10^5 k_r$,[f] s^{-1}
1	phosphate buffer	44.6	6.5	0.72			42.4 (11)	17.7 (18)	24.6 (25)
2	phosphate buffer	43.0	6.5	0.55			36.9 (14)	13.1 (14)	23.8 (25)
3	phosphate buffer	39.0	6.5	0.53	23.7 (17)	15.2 (15)	21.3 (8)	7.4 (2)	13.9 (2)
4	phosphate buffer	34.6	6.5	0.50	11.9 (13)		12.5 (5)	4.2 (6)	8.3 (12)
5	acetate buffer	34.5	4.7	0.62	10.3 (16)		10.0 (2)	3.8 (4)	6.2 (6)
6	phosphate buffer	34.6	3.5	0.53			9.7 (2)	3.3 (3)	6.4 (6)
7	nitric acid	33.5	2.3	0.60	10.5 (10)	12.7 (11)	10.4 (3)	3.9 (4)	6.5 (5)
8	$[Pt(en)(OH_2)_2]^{2+}$ (5×)	34.0	2.3	0.58			7.4 (3)	2.7 (3)	4.7 (5)
9	6-methyl-α-pyridone (5×)	35.4	6.5	0.61	9.3 (6)		12.9 (6)	4.8 (8)	8.1 (8)
10	α-pyridone (5×)	35.4	6.5	0.60	9.2 (5)	10.5 (5)	13.3 (3)	5.0 (5)	8.3 (8)
11	$DMSO/H_2O$ (10%)	36.2	6.5	0.52			9.7 (4)	3.3 (3)	6.4 (6)
12	phosphate buffer	26.4	6.5	0.59	2.5 (2)		3.2 (1)	1.2 (1)	2.0 (2)
13	tris buffer[e]	34.6	7.8	0.65			11.6 (5)	4.6 (5)	7.6 (8)

[a] Initial concentrations of **1** varied from 12.1 to 17.8 mM. [b] pH was maintained by 0.04 M phosphate buffer unless otherwise noted. [c] k_{obs}^1 and k_{obs}^2 for disappearance of the HH isomer resonances at −1601 and −2450 ppm, respectively, were calculated by using eq 3. The standard deviation for the fit in parentheses is much greater than that of k_{obs}^3 for several reasons. The signal-to-noise ratios for the HH isomer resonances were at most half of that for the HT isomer. In addition, the resonance at −2450 ppm was much broader, further decreasing the s/n. [d] Rate constant for the appearance of the HT resonance (δ = −2053 ppm) obtained from eq 4. [e] Additional resonances were observed; see text. [f] k_f and k_r were calculated by using the equations $k_{obs} = k_f + k_r$ and $K_{eq} = k_f/k_r$.

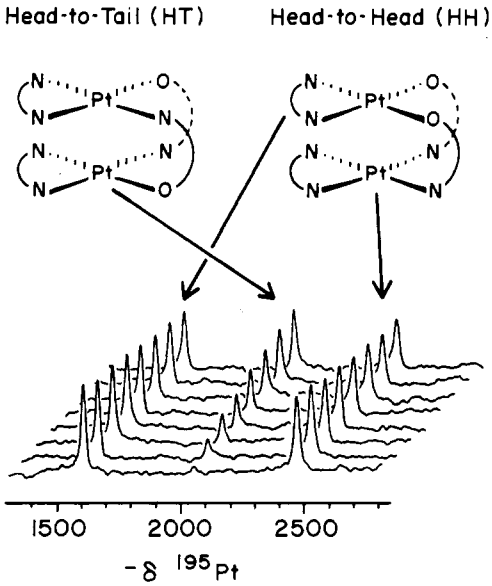

Figure 1. ^{195}Pt NMR spectra of an initial 17.9 mM solution of HH-$[Pt_2(en)_2(C_5H_4NO)_2](NO_3)_2$, pH 6.5 ($\mu$ = 60 mM (potassium phosphate buffer)), showing the time course of the isomerization reaction at 26.4 °C. The spectrum closest to the abscissa was taken after 0.43 h, and subsequent spectra were recorded after 3.6, 5.7, 7.8, 10.9, 13.1, 18.3, and 23.6 h.

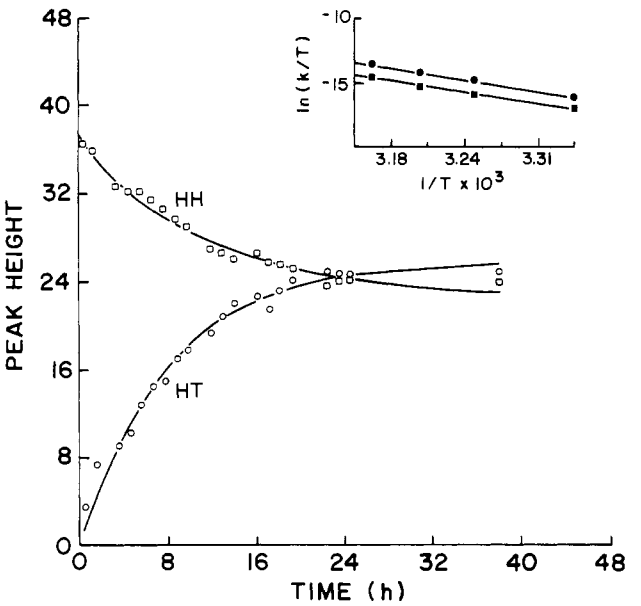

Figure 2. Peak height versus time curves for the data of Figure 1. The solid lines are the calculated appearance of the HT isomer, $x_t = x_e[1 - \exp(-k_{obs}t)]$, $k_{obs} = 3.23 \times 10^{-5}\ s^{-1}$, and disappearance of the HH isomer, $x_t = x_e + (x_0 - x_e)[\exp(-k_{obs}t)]$, $k_{obs} = 2.5 \times 10^{-5}\ s^{-1}$, from a least-squares fit to eq 3. An Eyring plot showing the temperature dependence of the rate constant is depicted in the inset.

(ethylenediamine)platinum(II) unit bound to an exocyclic oxygen of one bridging pyridonate ligand and a heterocyclic nitrogen of a second such ligand. The platinum atoms in the binuclear head-to-tail complex are equivalent, as schematically illustrated in Figure 1. Attempts to isolate the pure HT isomer (**2**) have thus far been unsuccessful (vide infra).

Kinetics Studies. The time dependence of the disappearance of the head-to-head isomer and the appearance of the head-to-tail isomer of **1** (Figure 1) is best fit to the integrated form of a rate law (eq 1) that describes a first-order approach to equilibrium (eq 2). The change in the peak height of either resonance of the

$$-d(HH)/dt = d(HT)/dt = k_f[HH] - k_r[HT] \quad (1)$$

$$HH \underset{k_r}{\overset{k_f}{\rightleftharpoons}} HT \quad (2)$$

HH isomer is directly proportional to the change in concentration with time, where $[HH]_0$ is the initial concentration of **1**. A typical fit to eq 3 of the time-dependent change in peak height of the

$$[HH]_t = [HH]_{eq} + ([HH]_0 - [HH]_{eq})[\exp(-(k_f + k_r)t)] \quad (3)$$

$Pt(N_2O_2)$ resonance (−1605 ppm) of the head-to-head isomer is given in the upper trace of Figure 2.

Similarly, the change in peak height of the ^{195}Pt resonance assigned as the head-to-tail isomer of **1** is proportional to half the concentration of this species; the time dependence of this change is given by eq 4. The lower trace of Figure 2 displays a typical

$$[HT]_t = [HT]_{eq}[1 - \exp(-(k_f + k_r)t)] \quad (4)$$

fit of data for the head-to-tail isomer to eq 4. Rate and equilibrium constants as functions of temperature, pH, solvent, added ligands, and mononuclear platinum species can be found in Table II.

The chemical shifts of both head-to-head and head-to-tail complexes of **1** show little (±4 ppm) or no dependence on temperature or pH (data not shown). An Eyring plot of temperature dependence of the rate constant (Figure 2), ln (k/T) vs $1/T$, reveals a large enthalpy of activation ($\Delta H^{\ddagger}$ = 114 (5) kJ/mol) and a small positive entropy of activation ($\Delta S^{\ddagger}$ = 40 (10)] J/(mol K)).

Distribution of Products and Mechanistic Studies. The only new ^{195}Pt resonance observed during the first 3 half-lives of runs 1–12 in Table II was that of the head-to-head isomer of **1**. At equilibrium, the solutions often revealed an extra peak at −2242

ppm, accounting for less than 10% of the platinum species. When the isomerization was studied at pH 7.8 in Tris buffer (run 13, Table II), additional resonances appeared at −2193 and −2250 ppm. After 4 half-lives, these resonances constituted 10 and 4%, respectively, of the total peak area. These resonances, plus one at −2746 ppm, were observed in an attempted run at pH 8.6, also in Tris buffer (data not shown). These peaks have similar intensity and, after 6 h, constitute 35% of the area of all platinum resonances. In this case, the isomerization was severely retarded and the product/reactant quotient ([HT]/[HH]) was 0.26 in comparison to the equilibrium value of 0.65 at pH 7.8 (run 13). Only the peak at −2242 ppm has been observed before in ^{195}Pt NMR studies of the (ethylenediamine)platinum(II)/α-pyridone system and is probably a hydroxide-bridged species.[19] The other three complexes have not been further characterized but may be reaction products of platinum(II) with Tris buffer.

Participation of solvent in the isomerization reaction was explored by following the rate and product distribution in 10% aqueous and neat DMSO solutions. Neither the rate nor the product distribution was affected in 10% DMSO in H_2O (run 11). The rate of isomerization was severely retarded, however, in the neat DMSO solution. After 10 h at 34.4 °C, most of the head-to-head isomer still was present, and the [HT]/[HH] ratio was less than ≈0.15. Under similar conditions in aqueous solution, the isomers would be equilibrated with a ratio of 0.6. In addition to being slower in neat DMSO, the isomerization reaction is accompanied by formation of mononuclear bis(α-pyridonato)-platinum(II) species, and two unidentified species with chemical shifts of −2356 and −2399 ppm appeared.

The failure to detect other platinum species by ^{195}Pt NMR spectroscopy during the course of kinetics studies in the pH range 2.3–6.5 suggests that mononuclear intermediates either are not involved in the isomerization or are present in only small, steady-state concentrations. To investigate the possible role of mononuclear complexes in the reaction mechanism, a 5-fold excess of $[Pt(en)(OH_2)_2]^{2+}$ was added (run 8, pH 2.3). The rate and product distributions were not significantly different from those of run 7, performed at the same temperature and pH but with no added $[Pt(en)(OH_2)_2]^{2+}$.

In another test of the involvement of mononuclear species, a 5-fold excess of free α-pyridone was added at pH 6.5. Under these conditions, α-pyridone readily attacks diaqua and dihydroxy-bridged species, yielding mono- and bis(α-pyridonate)-substituted complexes. These complexes can, in turn, dimerize, giving both HH and HT isomers of **1**.[20] During the approach to equilibrium, only ^{195}Pt resonances attributable to the HH and HT isomers appeared. When 6-methyl-α-pyridone was present in excess, spectra taken after 1 week (ca. 80 half-lives) revealed that 20% of the total ^{195}Pt peak area could be attributed to mononuclear bis(α-pyridonate/6-methyl-α-pyridonate) complexes.

Experiments with 6-methyl-α-pyridone also revealed that excess amounts of this ligand are not scrambled into the complex during the course of the isomerization. Binuclear (ethylenediamine)-platinum(II) complexes of 6-methyl-α-pyridonate have ^{195}Pt resonances shifted 25 ppm downfield relative to those of the α-pyridonate analogues. If 6-methyl-α-pyridonate were replacing α-pyridonate during isomerization of **1**, the HT peak would be expected to broaden and form a prominent low-field shoulder, depending on the extent of the substitution. Neither of these features was observed.

In a variation of the 6-methyl-α-pyridonate (6-Me-α-P) scrambling experiment, the HH and HT isomers of **1** were brought to equilibrium in the presence of the head-to-tail isomer of $[Pt_2(en)_2(6\text{-Me-}\alpha\text{-P})_2]^{2+}$ (cation of **5**). In contrast to the case for **1**, for which only the HH isomer was isolated, preparations of the analogue of **5** yielded only the HT isomer. The head-to-tail isomer of **5** was found not to isomerize over several months. ^{195}Pt NMR studies of the synthesis of **5** revealed the HH isomer to be formed only in miniscule amounts (<1%; data not shown), whereas similar studies of the synthesis of **1** and **2** showed the HH and HT isomers to be formed in approximately equal amounts.

Several attempts were made to measure the rate of isomerization of α-pyridonate-bridged *cis*-diammineplatinum(II) complexes. Samples of the head-to-head isomer, **3**, $[Pt_2(NH_3)_4(C_5H_4NO)_2](NO_3)_2$, and the head-to-tail isomer, **4**, $[Pt_2(NH_3)_4(C_5H_4NO)](NO_3)_2 \cdot 2H_2O$, were observed to isomerize in aqueous solution only over a period of several months at room temperature. Measurement of isomerization rates of the binuclear *cis*-diammineplatinum(II) complexes **3** and **4** is complicated, however, by the ease with which the HH isomer is oxidized to *cis*-diammineplatinum α-pyridone blue. All solutions of **3** and **4** were therefore purged with N_2 for 15 min prior to the beginning of a run. Isomerization of the HH *cis*-diammineplatinum(II) complex **3** was studied at 40 °C by ^{195}Pt NMR spectroscopy, but no HT isomer was detected after 10 h. This period represents ca. 11 half-lives in the isomerization of the HH (ethylenediamine)-platinum(II) complex at the same temperature. After 5 months at room temperature, there was a significant amount of the HT isomer present. The HT/HH ratio was 0.94 and approximately 10% of the platinum was present as the bis(α-pyridonato)platinum(II) monomer, indicating some decomposition of the binuclear complexes.

Attempts to measure the isomerization rate of **3** and **4** on a more reasonable time scale at 55 and 70 °C were hampered by a slow decomposition of the complexes both in phosphate buffer (pH 6.5) and unbuffered aqueous solutions. After several hours at 70 °C or several days at 55 °C, solutions of **3** gradually became blue/black and a black precipitate appeared. At 70 °C, the HT resonance disappeared with an initial first-order rate constant of 1.1×10^{-4} s^{-1}. The HH resonances initially increased but eventually reached a steady-state level representing approximately 20% of the initial platinum concentration. Since the HH complex is easily oxidized to a paramagnetic blue complex, we tentatively attribute the blue/black products to the decomposition of the HH complex, which disappears almost as fast as it is produced. Whether or not the HH or HT complex is decomposing, however, the initial first-order rate constant measured for the disappearance of the HT *cis*-diammineplatinum(II) α-pyridone complex establishes a lower limit for the rate of isomerization.

When the previously determined parameters for isomerization of the ethylenediamine complex **2** are used, the analogous rate constant, k_{-1}, is 8×10^{-3} s^{-1} at 70 °C. These results show that the isomerization rate of the HT α-pyridone complex of *cis*-diammineplatinum(II) with **4** is at least 70 times slower than the rate of HH ⇌ HT isomerization of the analogous (ethylenediamine)platinum(II) complexes. Since the main difference between the structurally characterized HH *cis*-diammineplatinum(II) and (ethylenediamine)platinum(II) complexes **3** and **1** is the torsional strain introduced by nonbonded steric interactions of the ethylenediamine rings in **1**, the 70-fold increase in the rate of HH and HT isomerization in the latter represents a steric acceleration of the rate-determining step.

Discussion

The ^{195}Pt NMR results clearly demonstrate the occurrence of a facile head-to-head to head-to-tail isomerization of the α-pyridonate-bridged binuclear complex, $[Pt_2(en)_2(C_5H_4NO)_2]^{2+}$ (**1**). An isomerization on this time scale was unexpected because it requires an unusually labile platinum–N(heterocycle) bond trans to an ammine nitrogen atom. These results may have some bearing on DNA-binding properties of the antitumor drug *cis*-DDP and the inactive trans isomer with the probable biological target DNA, chemistry that involves the formation of Pt–N(heterocycle) bonds.

Isomerization Is Reversible. The rate law (eq 1) was derived by assuming a reversible reaction (eq 2). The data do not fit a simple first-order expression unless the equilibrium condition is implicitly assumed in the rate law. Since the HT ethylenediamine isomer **2** could not be isolated, even though it was present in

(20) This point was established by monitoring with ^{195}Pt NMR spectroscopy the reaction of $[Pt(en)(OH_2)_2]^{2+}$ with α-pyridone (1/1) at pH 6.5. This reaction yields crystals of only the HH isomer. Both hydroxo-bridged and aqua hydroxo species are present initially but disappear over a 48-h period at 40 °C. Both HH and HT isomers form, and the [HH]/[HT] ratio is constant at ca. 0.6 throughout the reaction.

solution, an independent demonstration of the reverse reaction was not possible. However, both crystallographically characterized *cis*-diammineplatinum(II) α-pyridone isomers, **3** and **4**, were found to isomerize in separate ^{195}Pt NMR studies, demonstrating that both forward and reverse reactions can be traversed in an analogous system. Moreover, the −2055 ppm resonance can be unambiguously assigned to the HT isomer on the basis of the additivity of ^{195}Pt chemical shifts and information available about other possible solution species (Table I).

The magnitude of the rate and equilibrium constants in the (ethylenediamine)platinum(II) system suggest an explanation for our inability to isolate the HT isomer **2**. Assuming the solubility products of both isomers to be similar, and that the system can establish equilibrium as fast as the concentration is changed (rate of isomerization ≫ rate of crystallization), the isomer that precipitates will be the most concentrated one as determined by the equilibrium constant for eq 2, namely, the HH isomer. Since the ethylenediamine complex crystallizes over a period of several days upon evaporation of solvent in air, and the half-life for isomerization is approximately 7 h at room temperature, only the thermodynamically favored HH isomer is isolated. This relationship between the isomerization and crystallization rates explains why both the HH and HT *cis*-diammineplatinum(II) isomers, **3** and **4**, crystallize from the same solution. The rate of isomerization of **3** and **4** is much slower than the rate of crystallization. The solubility product of each isomer is exceeded before appreciable interconversion can occur and, therefore, both isomers can be isolated.

Dissociative Activation. Ligand exchange in Pt(II) complexes typically occurs via a five-coordinate intermediate in an associatively activated process.[21] Dissociative rate-determining steps, while rare in platinum(II) chemistry, are best documented for the cis–trans isomerization of $[Pt(PEt_3)_2(R)(X)]$ (R = alkyl or aryl; X = Cl, Br, etc.)[22] in the substitution of DMSO by bidentate ligands in *cis*-bis(aryl)bis(dimethyl sulfoxide)platinum(II) complexes.[23] Three lines of evidence support a rate-limiting dissociative step in the HH ⇌ HT isomerization of **1** and **2**:

First, the large enthalpy ($\Delta H^{\ddagger}$ = 114 (5) kJ/mol) and the small positive entropy ($\Delta S^{\ddagger}$ = 40 (10) J/(mol K)) of activation are characteristic of a dissociative bond-breaking step. Typically, platinum(II) substitution reactions exhibit much more negative $\Delta S^{\ddagger}$ values, ranging from −60 to −120 J/(mol K), and smaller values for $\Delta H^{\ddagger}$, from 60 to 100 kJ/mol.[24]

Second, the isomerization rate is drastically reduced in neat DMSO solution but is not affected in a 10% aqueous solution of DMSO. Since DMSO is a better nucleophile than water, acceleration of the rate in an aqueous DMSO solution would be expected for an associative, solvolytic activation step. Apparently, solvation of the departing group is important while platinum–solvent bond formation is not. A similar solvent role has been previously proposed to rationalize a dissociative k_1 substitution path.[25]

Finally, the HH ⇌ HT isomerization of **1** and **2** is sterically accelerated, also characteristic of rate-limiting dissociation. Studies of the HH and HT *cis*-diammineplatinum(II) complexes **3** and **4** reveal rates of isomerization at least 70 times slower than those of the more highly strained ethylenediamine dimers. Comparison of the X-ray crystal structures reveals two important changes in molecular geometry of the HH complexes upon replacing the *cis*-diammineplatinum(II) moieties with (ethylenediamine)platinum(II).[15] Nonbonded interactions between the ethylenediamine rings in adjacent coordination planes cause the Pt–Pt distance to increase from 2.877 (1) Å in **3** to 2.992 (1) Å in **1**. As the Pt–Pt distance increases, the two adjacent coordination planes must splay apart in order to accommodate the α-pyridonate ligand bite distance of 2.3 Å. Accordingly, the interplane tilt angle in the (ethylenediamine)platinum(II) complex is 9.6° greater than in the *cis*-diammineplatinum(II) analogue **3**. The adjacent platinum–ligand planes are twisted about the Pt–Pt axis toward a staggered conformation by an additional 4.6° relative to that for **3**. The torsional strain between the two interacting planes is manifest at their point of connection, the bridging α-pyridonate ligand. Apparently, this strain accelerates the Pt–α-pyridonate dissociation. When one Pt–α-pyridonate bond is broken, the strain is relieved and the complex is free to rearrange or to undergo further dissociation. A similar effect of steric strain was also observed previously to affect the redox chemistry of these compounds.[26]

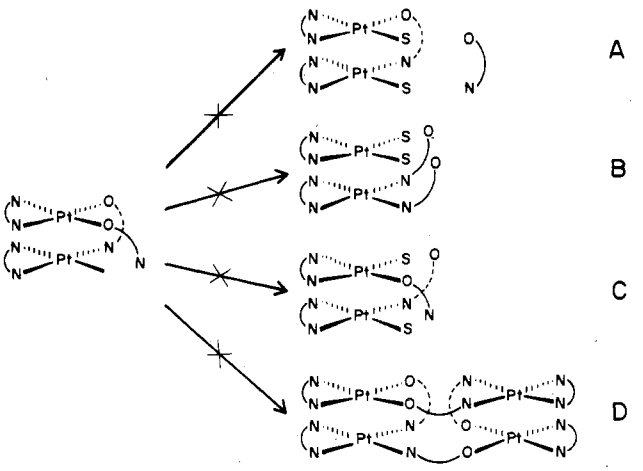

Figure 3. Schematic diagram of four possible intermolecular paths for the HH ⇌ HT isomerization following an initial dissociative rate-determining step (S = solvent).

Isomerization Is Intramolecular. The unimolecular rate-determining step involves disruption of a platinum–α-pyridonate bond. If another such bond is broken before the bridge is reformed, the isomerization proceeds through an intermolecular path. Figure 3 shows four possible intermolecular paths that have been eliminated by competition and scrambling experiments.

Following an initial dissociative step, rupture of the bond between the same α-pyridonate ligand and the second platinum atom would result in complete dissociation of this bridging ligand from the binuclear complex. This possibility was tested by adding the diaqua(ethylenediamine)platinum(II) complex **6** to a solution of the HH complex and following the rate of isomerization. The labile complex **6** will compete with binuclear species (Figure 3A) for any free α-pyridonate ligand, producing observable mononuclear α-pyridone complexes and altering the rate of approach to equilibrium. Comparison of rate and equilibrium constants for runs 7 and 8 in Table II reveals no significant effect of **6** on the HH ⇌ HT isomerization, nor were any mononuclear species observed by ^{195}Pt NMR spectroscopy in the course of isomerization. Complementary studies with a 5-fold excess of the α-pyridone and 6-methyl-α-pyridone free ligands at a pH for which α-pyridone reacts readily with aquaplatinum(II) complexes also reveal no significant change in product distribution or rate or equilibrium constants for the isomerization reaction (runs 9 and 10 vs run 4, Table II).

Studies on the reaction in the presence of free 6-methyl-α-pyridone (Table II, run 9) provide a nonkinetic scrambling test for the presence of totally dissociated ligand. Since the chemical shifts of the HT isomers of bridged binuclear (6-methyl-α-pyridonato)- and (α-pyridonato)(ethylenediamine)platinum(II) complexes differ by ≈25 ppm, a mixed complex would be observed at equilibrium. The only new ^{195}Pt NMR peak was that of the HT isomer of **2** (δ = −2055), however, and no shoulder was

(21) Basolo, F.; Pearson, R. G. *Mechanisms of Inorganic Reactions*; Wiley: New York, 1967; p 387.
(22) Romeo, R.; Minniti, D.; Lanza, S. *Inorg. Chem.* **1979**, *18*, 2362.
(23) Lanza, S.; Minniti, D.; Romeo, R.; Moore, P.; Sachinidis, J.; Tobe, M. *J. Chem. Soc., Chem. Commun.* **1984**, 543.
(24) See ref 21, p 405.
(25) Faraone, G.; Ricevuto, V.; Romeo, R.; Trozzi, M. *Inorg. Chem.* **1969**, *8*, 2207; **1970**, *9*, 1525.
(26) (a) O'Halloran, T. V.; Roberts, M. M.; Lippard, S. J. *Inorg. Chem.* **1986**, *25*, 957. (b) O'Halloran, T. V.; Mascharak, P. K.; Williams, I. D.; Roberts, M. M.; Lippard, S. J. *Inorg. Chem.* **1987**, *26*, 1261.

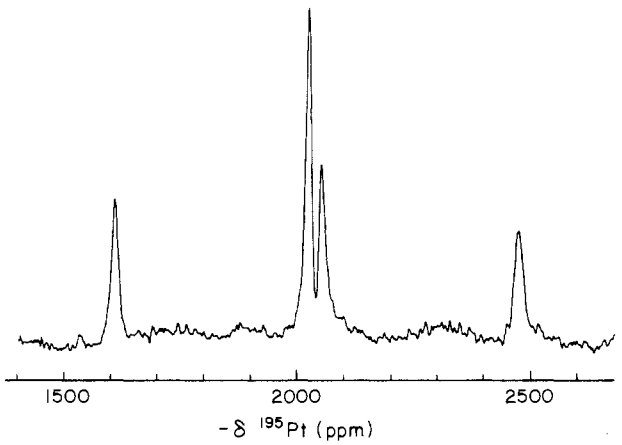

Figure 4. ^{195}Pt NMR spectrum of a mixture of the HH isomer of $[Pt(en)(C_5H_4NO)]_2^{2+}$ and the HT isomer of $[Pt(en)(6\text{-Me-}\alpha\text{-P})]_2^{2+}$ after ca. 200 h at 25 °C. No scrambling of bridging ligands between the binuclear complexes is observed, even after the α-pyridonate-bridged isomers have equilibrated. This spectrum is the sum of 333 160 transients and was accumulated by using a spectral width of 100 kHz and a pulse width of 6 μs (21°).

observed on this resonance even after 9 half-lives. The above results also rule out complete dissociation of platinum subunits, as illustrated in Figure 3B,C.

Finally, the possibility of an intermolecular path involving dimerization of two bridged binuclear complexes was explored (Figure 3D). A binuclear process of this nature was proposed to account for the isomerization of Schiff base nickel(II) complexes.[27] This possibility was eliminated for eq 2 on the basis of experiments in which the HT isomer of $[Pt(en)_2(6\text{-Me-}\alpha\text{-P})_2]_2^{2+}$ (cation of **5**) was added during the equilibration of the HH and HT isomers of **1** and **2**. If the binuclear pathway in Figure 3D occurred following initial dissociation, mixed-ligand complexes should have been observed by ^{195}Pt NMR spectroscopy. Figure 4 reveals resonances for two HT complexes **2** and **5** that are well resolved, demonstrating that the mixed-ligand complexes, if present, represent less than 5% of the total platinum species present.

Postulated Mechanism. With the major intermolecular paths ruled out, the following sequence of reactions is postulated to account for the HH ⇌ HT isomerization: initial dissociative step; rapid intramolecular, linkage isomerization; and, finally, bond formation between the uncoordinated end of the ligand and the platinum center involved in the initial dissociative step. Scheme IA shows such a process where the Pt–N bond of the HH complex is cleaved initially, while scheme IB reveals the analogous path with initial Pt–O bond breaking (Figure 5).

The forward rate constant k_f, derived from eq 3 and 4, can be assigned to either the k_1 or k_1' step of Figure 5. Independent measurements of the initial rate constant (k_i) for the disappearance of the HH isomer and the appearance of the HT isomer reveal that k_i is equal to k_f within experimental error in both cases.[19] This result is consistent with the $k_f = k_1$ (or k_1') assignment. Assignment of k_f to the linkage isomerization step k_2 is not consistent with the dual constraints of dissociative activation and the intramolecular path.

Finally, k_r can be assigned to k_{-3} or k_{-1}/K_2K_3, or the corresponding steps in Scheme IB, where $k_2/k_{-2} = K_2$ and $k_3/k_{-3} = K_3$. Since the HT isomer could not be isolated, initial rate data are not available to check this assignment. Because there is no evidence for intermediates or additional equilibria in the HH ⇌ HT isomerization, the mechanisms in scheme I are best considered as concerted I_d, with bond breaking playing the most important role in the transition state. Since the observed forward and reverse rate constants are related by the equilibrium constant (eq 2), the principle of microscopic reversibility restricts their assignment to mechanism IA or IB, unless an identical transition state is common

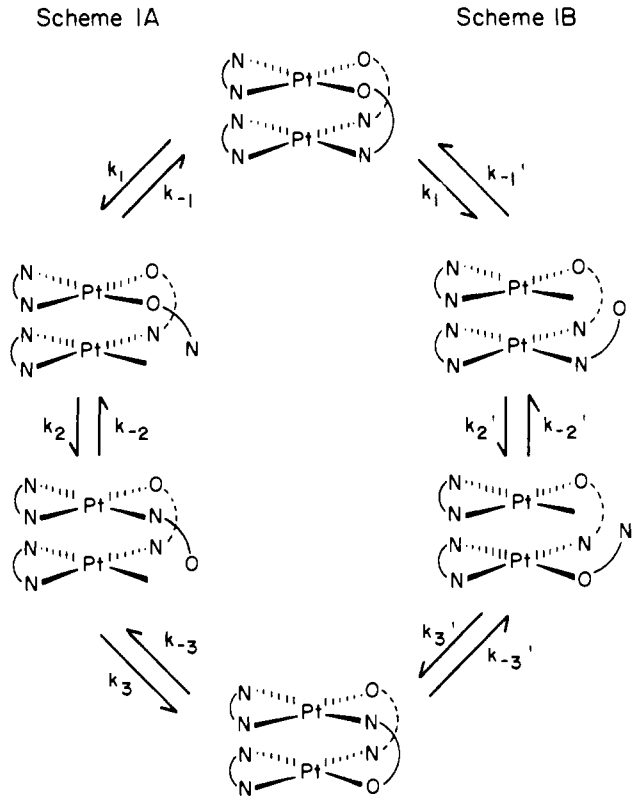

Figure 5. Two reversible, intramolecular mechanisms for the HH ⇌ HT isomerization. Scheme IA represents a sequence of reactions if the initial rate-determining step involves Pt–N(pyridonate) bond breaking in the head-to-head (HH) isomer. Scheme IB represents a similar sequence of reaction if Pt–O(pyridonate) bond breaking in the HH isomer is the initial step.

to both pathways.[28] We argue that scheme IA better represents the isomerization mechanism than scheme IB for two reasons. First, inspection of Table II reveals K_{eq} to be ca. 0.6 under most conditions; therefore, the observed forward rate constants (k_f) are 60% smaller than the reverse rate constants (k_r). Considering that Pt–N(heterocycle) bonds trans to an ammine ligand are more inert than Pt–O bonds, the slower forward rate constant is better assigned to the Pt–N versus Pt–O bond breaking, k_1 step of scheme IA. Another reason for preferring Scheme IA is that the alternative scheme IB may involve unfavorable steric interactions in the steps involving reorientation of the bridging ligand. In the course of such a linkage isomerization, one bridging ligand must rotate by 180°. Study of CPK space-filling models reveals that such rotation of the α-pyridonate ligand about the Pt–N(α-pyridonate) bond in the HH isomer is restricted by the proximity of the second pyridonate ring. This barrier is less significant in scheme IA, where the ligand rotates about a Pt–O bond in the HH isomer.

Conclusions

The HH ⇌ HT isomerization requires an unusually facile postulated cleavage of a Pt(II)–N(heterocycle) bond trans to an ammine ligand. Kinetic and other tests reveal this rearrangement to be reversible, intramolecular, and dissociatively activated. Studies of analogous HH and HT *cis*-diammineplatinum(II) α-pyridonate complexes of $[Pt(NH_3)_2(C_5H_4NO)]_2^{2+}$ reveal a drastically reduced rate of isomerization and therefore a presumably more inert Pt–N(heterocycle) bond. Accordingly, enhanced lability of the Pt–N(heterocycle) bond is not attributed to the nature of bridged binuclear complexes per se but to increased torsional strain introduced by nonbridging ligand steric interactions. The present results show that steric factors can dramatically affect the lability of typically inert and thermodynamically stable

(27) Reference 21, p 430.

(28) Moore, J. W.; Pearson, R. G. *Kinetics and Mechanisms*; Wiley: New York, 1981; p 372.

platinum–nitrogen bonds. Such factors may also affect the binding of platinum(II) ammine complexes with the heterocyclic bases in DNA, as additional work has recently revealed.[29]

Acknowledgment. This work was supported by PHS Grant CA 34992 awarded by the National Cancer Institute, DHHS. We thank Dr. P. Mascharak for helpful discussions and Engelhard Industries for a generous loan of K_2PtCl_4, from which the platinum complexes were prepared.

(29) Comess, K.; Lippard, S. J. To be submitted for publication.

Registry No. $[Pt_2(en)_2(C_5H_4NO)_2]^{2+}$, 85370-19-0; ^{195}Pt, 14191-88-9.

Contribution from the Department of Chemistry, University of Southern California, Los Angeles, California 90089-0744

Restudy of the Action of Sulfur Dioxide on Dry Trimethylamine Oxide: Iodine Oxidation and Lewis Acid Chemistry of the Most Reactive Product, $(CH_3)_2(H)NCH_2SO_3$

Anton B. Burg

Received July 6, 1988

Further study of the action of SO_2 on dry $(CH_3)_3NO$ has led to new chemistry of $(CH_3)_2(H)NCH_2SO_3$ ("KS8")—often the major product but sometimes exceeded by $(CH_3)_3NSO_3$, with small yields of $(CH_3)_3NH^+$. X-ray study of a single crystal (monoclinic) of KS8 showed the space group $P2_1/c$, with 12 molecules per unit cell: V = 1860 (1) Å^3, a = 12.069 (5) Å, b = 12.434 (6) Å, c = 13.413 (6) Å, and β = 112.50 (3)°. The nontetrahedral angles are O–S–C = 105.3°, O–S–O = 113.5°, and S–C–N = 112.7°. Aqueous iodine oxidizes KS8 (with first-order kinetics) to give SO_4^{2-}, 2 I^-, 3 H^+, and presumably $(CH_3)_2(H)NCH_2OH^+$. Attempts to stabilize the presumed initial product $(CH_3)_3NOSO_2$ by attaching HCl or BF_3 below −78 °C led only to the Lewis-acid chemistry of KS8. With HCl at 70 °C, KS8 quantitatively liberates SO_2, forming $(CH_3)_2NH_2Cl$, H_2O, the known salt $(CH_3)_2N{=}CH_2{}^+Cl^-$ ("CDMA"), $x H_2CO{\cdot}HCl$, and yCDMA·HCl. CDMA was identified by X-ray study of a single (orthorhombic) crystal. Its space group is *Pmmn* with two molecules per unit cell: V = 244.4 (1) Å^3, a = 6.198 (2) Å, b = 7.034 (3) Å, c = 5.607 (1) Å, and $\alpha = \beta = \gamma = 90°$. Cl^- is coplanar with NC_3 units. CDMA or KS8 with HCl in liquid SO_2 forms polymers and a product conjectured to be $(CH_3)_2NCH_2SO_2Cl$. KS8 with BF_3 at 55 °C quantitatively liberates SO_2; then the ^{13}C NMR spectrum indicates the product to be $(CH_3)_2(H)NCH_2O{\cdot}2BF_3$. Solvent acetone removes the BF_3 from this, forming what seems to be $(CH_3)_2NCH_2OH$. Peripheral aspects seem worthy of further study.

The original study of the action of SO_2 on very well dried $(CH_3)_3NO$ at low temperatures gave a main product believed to be $(CH_3)_3NOSO_2$, with two lines of physical evidence suggesting as much as 20% of the relatively inert isomer $(CH_3)_3NSO_3$,[1] soon confirmed elsewhere.[2] The obvious structure $(CH_3)_3NOSO_2$ was contradicted many years later,[3] but the correct structure $(CH_3)_2(H)NCH_2SO_3$ (now confirmed by X-ray crystallography) was recognized only very recently, by King and Skonieczny,[4] who called it product 8; hence it is called hereafter "KS8". However, ref 3 and 4 do not mention $(CH_3)_3NSO_3$; its ^1H NMR singlet is covered by the doublet for CH_3 in KS8.

The present study has shown that even a very slow addition of SO_2 to $(CH_3)_3NO$ (as the solid or in solution) at temperatures as low as −100 °C gives KS8 with yields of $(CH_3)_3NSO_3$ seldom less than 15%, but sometimes more than 50%, most cleanly determined by the ^{13}C NMR spectrum of the mixture. Such results seem to require reconsideration of the suggested reaction mechanism.[4]

It seems reasonable to suggest that the initial formation of $(CH_3)_3NOSO_2$ provides far more than enough energy to cleave the N–O bond even at −100 °C. Then the side-by-side $(CH_3)_3N$ and SO_3 would directly form $(CH_3)_3NSO_3$ or sulfonation at a C–H bond would give KS8. Some of the protons from this sulfonation would account for minor yields (near 8%) of $(CH_3)_3NH^+$. However, if $(CH_3)_3NOSO_2$ ever could be made by a low-energy process, it might well rearrange in the Polonovski manner;[4] then $(CH_3)_3NSO_3$ might well be absent.

If the presumed initial product $(CH_3)_3NOSO_2$ could go to KS8 only by a Polonovski-like rearrangement,[4] this process might be slow enough at −78 °C or lower to permit stabilization by Lewis acids, forming secondary adducts such as $(CH_3)_3NOSO_2{\cdot}HCl$ and $(CH_3)_3NOSO_2{\cdot}BF_3$—expected because the N–O oxygen would enhance the base action of the S–O oxygen, just as addition of O^{2-} to SO_2 makes the stronger base SO_3^{2-}. However, numerous attempts failed to produce such adducts even at −100 °C. Warmed with HCl or BF_3, the low-temperature product showed only the chemistry of KS8, with $(CH_3)_3NSO_3$ and $(CH_3)_3NH^+$ inert.

This Lewis-acid chemistry includes the action of HCl on solid KS8 to form the interesting salt $(CH_3)_2N{=}CH_2{}^+Cl^-$ or on the SO_2 solution to form the conjectured $(CH_3)_2NCH_2SO_2Cl$, and the action of BF_3 on solid KS8 to form $(CH_3)_2(H)NCH_2O{\cdot}2BF_3$. Other Lewis acids also could have interesting consequences. Also, the first-order oxidation of KS8 by KI_3 opens the study of KS8 as a reducing agent.

Experimental Methods

Chemical Procedures. All volatile reagents, reactants, solvents, and products were managed in a relatively simple Stock-type high-vacuum system, permitting quantitative work with complete exclusion of moisture. Nonvolatiles were brought to reaction in tubes like those shown in Figure 1, often modified for specific purposes. For example, a tube of type A, with the neck a lengthened to facilitate sealing off and reopening to the vacuum line, was used for the action of HCl (at 5 atm pressure and 70 °C) on KS8 in chamber d. After removal of the volatiles to the vacuum line for separation and measurement, the CDMA was sublimed to chamber ab, next sealed off at b. Solvent SO_2 was brought in and neck a sealed off again; now the SO_2 solution of CDMA was poured into the NMR tube, to be sealed off with the sample at −196 °C. The less volatile sublimate $(CH_3)_2NH_2Cl$ was managed in the same way.

Tubes of type **B** were used for the action of SO_2 on $(CH_3)_3NO$ dissolved in $HCCl_3$, H_2CCl_2, or HCF_2Cl. The amine oxide was dehydrated by evacuation at 25 °C (16 h) and resublimation until no more water came to the U-trap at −196 °C. Any sublimate that reached the upper bulb could be washed down by refluxing the solvent. After the SO_2 reaction, the suspended precipitate could be pipetted into an NMR tube

(1) Burg, A. B. *J. Am. Chem. Soc.* **1943**, *65*, 1633.
(2) Lecher, H. Z.; Hardy, W. B. *J. Am. Chem. Soc.* **1948**, *70*, 3789.
(3) Craig, J. C.; Purushothaman, K. K. *Tetrahedron Lett.* **1969**, *60*, 5305.
(4) King, J. F.; Skonieczny, S. *Phosphorus Sulfur* **1985**, *25*, 11.

0020-1669/89/1328-1295$01.50/0 © 1989 American Chemical Society